Temperature-Dependent Photoelectron Spectroscopy of Methyl Benzoate Anions: Observation of Steric Effect in *o*-Methyl Benzoate†

Hin-Koon Woo, Xue-Bin Wang, Boggavarapu Kiran, and Lai-Sheng Wang*

Department of Physics, Washington State University, 2710 University Drive, Richland, Washington 99352, and W. R. Wiley Environmental Molecular Sciences Laboratory and Chemical Sciences Division, Pacific Northwest National Laboratory, MS 8-88, P.O. Box 999, Richland, Washington 99354

Received: June 2, 2005; In Final Form: August 10, 2005

Temperature-dependent photoelectron spectra of benzoate anion ($C_6H_5CO_2^-$) and its three methyl-substituted isomers (*o*-, *m*-, *p*-$CH_3C_6H_4CO_2^-$) have been obtained using a newly developed low-temperature photoelectron spectroscopy apparatus that features an electrospray source and a cryogenically controlled ion trap. Detachment channels due to removing electrons from the carboxylate group and benzene ring π electrons were distinctly observed. Well-resolved vibrational structures were obtained in the lower binding energy region due to the OCO bending modes, except for *o*-$CH_3C_6H_4CO_2^-$, which yielded broad spectra even at the lowest ion trap temperature (18 K). Theoretical calculations revealed a large geometry change in the OCO angles between the anion and neutral ground states, consistent with the broad ground-state bands observed for all species. A strong steric effect was observed between the carboxylate and the methyl group in *o*-$CH_3C_6H_4CO_2^-$, such that the $-CO_2^-$ group is pushed out of the plane of the benzene ring by ~25° and its internal rotational barrier is significantly reduced. The low rotational barrier in *o*-$CH_3C_6H_4CO_2^-$, which makes it very difficult to be cooled vibrationally, and the strong coupling between the OCO bending and CO_2 torsional modes yielded the broad PES spectra for this isomer. It is shown that there is *no* C−H···O hydrogen bond in *o*-$CH_3C_6H_4CO_2^-$, and the interaction between the carboxylate and methyl groups in this anion is found to be repulsive in nature.

1. Introduction

Methyl-substituted benzoic acids have been one of the classical examples for demonstrating the steric effect of the methyl group in physical organic chemistry.[1,2] The steric effect is often divided into several components, namely, primary steric effect, steric inhibition to resonance, and hydrogen bonding.[3,4] The existence of intramolecular hydrogen bond in methyl-substituted benzoic acid has been proposed to explain the stronger acidity of the ortho-isomer;[5−7] in the anions intramolecular C−H···O hydrogen bond has been assumed to form between the methyl hydrogen and the carboxylate oxygen in *o*-$CH_3C_6H_4CO_2^-$.[5] Indeed this type of weak C−H···O hydrogen bond has been recognized to play important roles in chemistry, biochemistry, and materials science.[8−13] It has been identified in solid-state physics,[9] crystal engineering,[14−17] and biological systems.[18−21] The ability for a C−H group to be a hydrogen bond donor is found to be dependent on the hybridization of the carbon atom. The hydrogen bond strength decreases in the order, $C(sp)-H > C(sp^2)-H > C(sp^3)-H$.[22,23] Hence, the hydrogen bond formed by a methyl (CH_3) donor is expected to be the weakest. Nevertheless, it plays important roles in chemistry and needs to be understood. Yet as of this date, experimental characterizations on C−H···O hydrogen bonding with a CH_3 donor are rather scarce.

Using a newly developed low-temperature photoelectron spectroscopy (PES) apparatus,[24] which features an electrospray ionization (ESI) source and a temperature-controlled ion trap, we have recently investigated weak C−H···O hydrogen bonding in a series of aliphatic carboxylate molecules, $CH_3(CH_2)_nCO_2^-$ ($n = 0-8$), involving the terminal methyl group and the carboxylate group.[25] Under low-temperature conditions, C−H···O hydrogen-bonds were observed to form between the terminal $-CH_3$ group and the $-CO_2^-$ group for $n > 4$, inducing a linear to folded structural transformation. The negative charge on the carboxylate was observed to be stabilized significantly at low temperatures relative to that at room temperature due to the C−H···O hydrogen bond in the folded conformation. The strengths of the C−H···O hydrogen bonds have been experimentally characterized to be from 1.2 to 4.4 kcal/mol, on the basis of the electron binding energy shifts of the carboxylate group.[25]

In the current study, we extend the C−H···O hydrogen bond investigation to methyl-substituted benzoic acid systems. We hypothesized that *o*-$CH_3C_6H_4CO_2^-$ should exhibit a higher electron binding energy relative to the meta- and para-isomers due to the C−H···O hydrogen bonding, which is expected to stabilize the negative charge on the $-CO_2^-$ group. We have measured temperature-dependent PES spectra of the three isomers of the methyl-substituted benzoate anions as well as benzoate as a control experiment at two photon energies (266 and 193 nm) and three ion trap temperatures (300, 70, and 18 K). Similar spectral patterns were observed for all four species. Well resolved vibrational structures were observed in the 266 nm spectra at all temperatures, except for *o*-$CH_3C_6H_4CO_2^-$, for which vibrational features were only observed at the lowest ion trap temperature. Surprisingly, the electron binding energies of *o*-$CH_3C_6H_4CO_2^-$ was not higher than the meta- and para-isomers. We found that there is *no* C−H···O hydrogen bonding

† Part of the special issue "Jack Simons Festschrift".

* To whom correspondence should be addressed. E-mail: ls.wang@pnl.gov.

10.1021/jp0529467 CCC: $30.25
Published on Web 09/21/2005

in *o*-$CH_3C_6H_4CO_2^-$. In fact, a strong steric effect (repulsive interactions) was observed between the $-CH_3$ and $-CO_2^-$ groups in the ortho-isomer, which pushes the $-CO_2^-$ group out of the benzene ring and significantly reduces its internal rotational barrier. Our experimental observation is confirmed by theoretical calculations.

2. Experimental and Theoretical Methods

2.1. Low-Temperature ESI−PES. The ESI source and the magnetic bottle PES analyzer used in the newly developed low-temperature apparatus is similar to that previously described.[26] A key feature of the new apparatus is a temperature-controlled ion trap that is used for ion accumulation and cooling.[24] The ion trap is attached to the cold head of a closed-cycle helium refrigerator, which can reach a low temperature of 10 K and can be controlled up to 350 K. The anions of interests, $C_6H_5CO_2^-$ and *o*-, *m*-, and *p*-$CH_3C_6H_4CO_2^-$, were produced using the ESI source from $\sim 1.0 \times 10^{-3}$ mol solutions of the corresponding acids in a mixture of methanol/water solvent (3/1 volume ratio). Anions produced were guided by a RF-only octople into a quadruple mass filter operated in the RF-only mode. Following the mass filter, ions were directed by a 90° ion bender to the temperature-controlled ion trap, where they were accumulated and cooled via collisions with a background gas. Background gases used are N_2 for the temperature range between 350 and 70 K, while for lower temperatures down to 10 K, a mixture of 20% H_2 in helium is used. Ions were trapped and cooled for a period of 20−80 ms before pulsed into the extraction zone of a time-of-flight mass spectrometer at a repetition rate of 10 Hz.

During the PES experiment, ions were mass-selected and decelerated before being intercepted by a probe laser beam in the photodetachment zone of the magnetic bottle photoelectron analyzer. Two detachment photon energies were used in the current experiment: 266 nm (4.661 eV) from an Nd:YAG laser and 193 nm (6.424 eV) from an ArF excimer laser. The lasers were operated at a 20 Hz repetition rate with the ion beam off at alternating laser shot for shot-by-shot background subtraction. Photoelectrons were collected at nearly 100% efficiency by the magnetic bottle and analyzed in a 5.2-m-long electron flight tube. Time-of-flight photoelectron spectra were collected and converted to kinetic energy spectra, calibrated by the known spectra of I^- and ClO_2^-.[27] The electron binding energy spectra were obtained by subtracting the kinetic energy spectra from the detachment photon energy used. The energy resolution ($\Delta E/E$) was about 2% (i.e., ~20 meV for 1 eV electrons).

2.2. Theoretical Methods. Density functional theory (DFT) was used to determine the geometry and electronic structure of the benzoate anion, the three methyl-substituted benzoate anions, and their corresponding neutrals. Geometry optimizations were calculated using the hybrid B3LYP[28] exchange-correlation functional and the 6-31+G** basis set. We calculated the frequencies for all species to verify that the geometries were minima on the potential energy surface. The only significant conformation flexibility involves rotation of the carboxylate groups. We explored these rotations and found only one stable conformer of each anion and the corresponding neutral. The adiabatic detachment energies (ADEs) of the anions were obtained by taking the energy difference between the anions and the ground state of the neutrals in its optimized geometry. All of the DFT calculations were carried out with Gaussian 03.[29]

3. Experimental Results

3.1. Photoelectron Spectra at 266 nm. Figure 1 shows the 266 nm PES spectra of the four anions at three ion trap temperatures. The binding energy scale is plotted starting from 3.0 to 4.6 eV for clearer presentation because there is no detachment transition below 3 eV (see Figure 2). Spectra for all four anions exhibit similar spectral patterns and binding energies, all due to detachments from primarily $-CO_2^-$ derived molecular orbitals (see section 5.1),[30] but their vibrational fine features are quite different. At room temperature, similar and partially resolved vibrational structures were already discernible for $C_6H_6CO_2^-$, *m*-$CH_3C_6H_4CO_2^-$, and *p*-$CH_3C_6H_4CO_2^-$. At 70 K, the vibrational structures were significantly better resolved due to the vibrational cooling in the anions. At the lowest ion

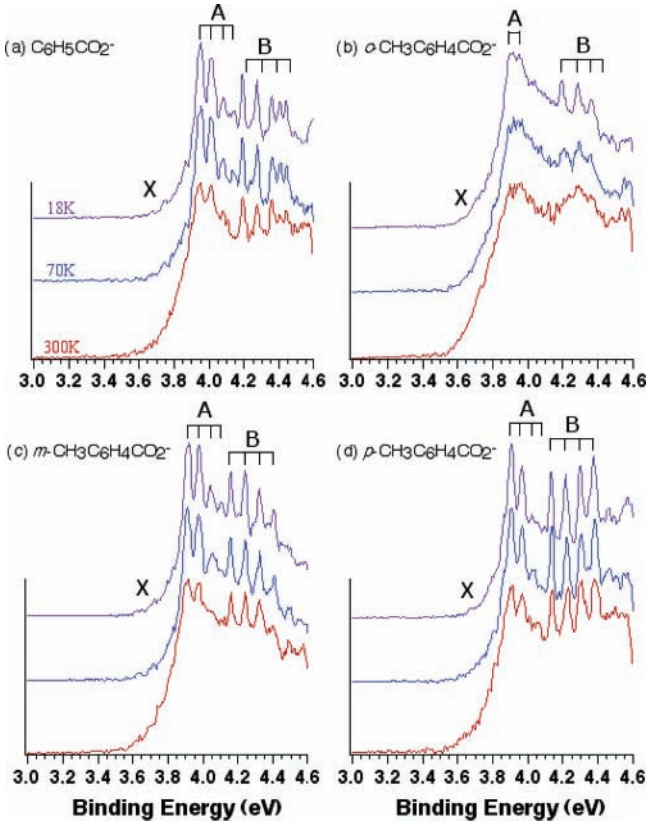

Figure 1. Photoelectron spectra of (a) $C_6H_5CO_2^-$, (b) *o*-$CH_3C_6H_4CO_2^-$, (c) *m*-$CH_3C_6H_4CO_2^-$, and (d) *p*-$CH_3C_6H_4CO_2^-$ at 266 nm (4.661 eV) and three different ion trap temperatures. Red, 300 K; blue, 70 K; purple, 18 K.

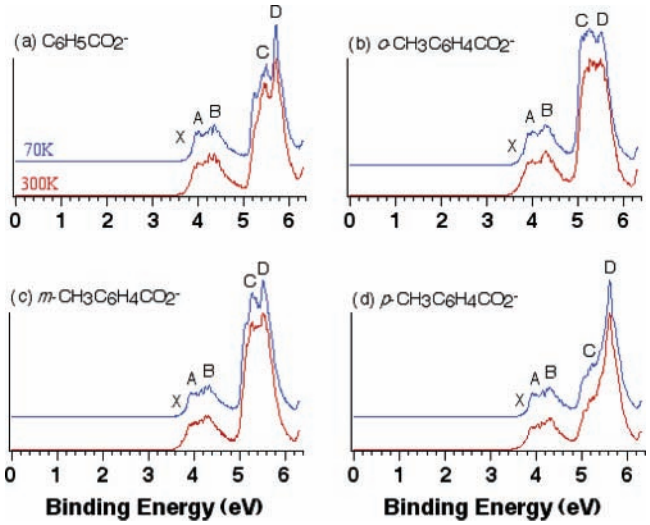

Figure 2. Photoelectron spectra of (a) $C_6H_5CO_2^-$, (b) *o*-$CH_3C_6H_4CO_2^-$, (c) *m*-$CH_3C_6H_4CO_2^-$, and (d) *p*-$CH_3C_6H_4CO_2^-$ at 193 nm (6.424 eV) and two different ion trap temperatures. Red, 300 K; blue, 70 K.

TABLE 1: Experimental and Theoretical Adiabatic Detachment Energies (ADE), Vertical Detachment Energies (VDE), and Vibrational Frequencies of the OCO Bending Mode

		ADE (eV)			VDE (eV)[a]	vib. frequency (cm^{-1})[a]
		exp[a]	theor	EA[b]		
$C_6H_5CO_2^-$	X	3.59 (5)[c]	3.44	3.45 ± 0.16		
	A	3.95 (1)				480 (20)
	B	4.19 (1)				640 (20)
	C	5.14 (2)			~5.4	
	D				5.72 (2)	
o-$CH_3C_6H_4CO_2^-$	X	3.55 (5)[c]	3.35	3.48 ± 0.16		
	A	3.90 (2)				480 (40)
	B	4.19 (1)				640 (20)
	C	4.96 (2)			~5.3	
	D				5.52 (6)	
m-$CH_3C_6H_4CO_2^-$	X	3.61 (5)[c]	3.40	3.43 ± 0.16		
	A	3.92 (1)				480 (20)
	B	4.16 (1)				640 (20)
	C	4.99 (2)			~5.3	
	D				5.52 (2)	
p-$CH_3C_6H_4CO_2^-$	X	3.62 (5)[c]	3.37	3.41± 0.16		
	A	3.91 (1)				480 (20)
	B	4.14 (1)				640 (20)
	C	4.87 (2)			~5.2	
	D				5.63 (20)	

[a] Numbers in parentheses are uncertainties in the last digits. [b] Electron affinities estimated from thermodynamic cycles from ref 34. [c] Threshold detachment energy (TDE), representing the upper limit for ADE. See text.

trap temperature of 18 K, the vibrational structures were not significantly improved, suggesting that the vibrational cooling was already sufficient even at 70 K. However, the fine features of the *o*-$CH_3C_6H_4CO_2^-$ spectra are completely different. At room temperature, no vibrational structures were resolved. At 70 K, fine features were only discernible for the B band. Only at the lowest ion trap temperature (18 K) were we able to resolve the vibrational structures in the B band, whereas vibrational fine features were still just barely visible for the A band. The vibrational frequencies for the A and B bands characteristic of the OCO bending mode are identical for all species within our experimental accuracy: 480 cm^{-1} for the A band and 640 cm^{-1} for the B band (Table 1).

A long tail was observed at the lower binding energy side in all the spectra. Low binding energy tails in PES spectra are usually due to hot band transitions and should be eliminated for vibrationally cold anions, as we have shown for a relatively large anion, C_{60}^-.[31] However, the low energy tail was present in the PES spectra of all the four benzoate anions even at the lowest temperature of 18 K, at which we expected all vibrational hot bands to be eliminated. This observation suggests that an electronic transition with a very broad Franck−Condon progression was present in the low binding energy side. This transition (X) should correspond to the ground state of the neutral species, and the A and B bands should then correspond to detachment transitions to the first and second excited states of the neutrals, respectively. Therefore, our PES spectra suggest that there must be a large geometry change between the anion and neutral ground states for all the four benzoate species, which is confirmed by our theoretical calculations (see below). In this case, the threshold detachment energies (TDEs) may not represent the ADEs or the electron affinities (EAs) of the neutral species because the Franck−Condon factors for the 0−0 transitions may be negligible. Instead, the TDEs should be considered as the upper limits for the ADEs. Due to the low signal-to-noise ratio and lack of vibrational resolution in the lower binding energy region, we were only able to estimate the TDEs from the onset of appreciable photoelectron signals. The TDEs so estimated for the ground-state transitions and the ADEs and vibrational frequencies obtained for the A and B states are given in Table 1 for all four species.

3.2. Photoelectron Spectra at 193 nm. Figure 2 displays the 193 nm photoelectron spectra of the four anions at two ion-trap temperatures. Additional features due to detachments from the π electrons of the benzene ring were observed at higher binding energies (see section 5.1).[30] The low-temperature spectra show slightly better resolved peaks than the room temperature spectra in the higher binding energy part of the spectra, which seem to contain fine features and their relative intensities seem to be different in the four spectra. The electron binding energies of the C and D bands are also given in Table 1. We note that the relative intensities of the carboxylate-derived bands are considerably weaker than those derived from the ring π electrons. We found previously that these features are highly photon energy dependent: at 157 nm the relative intensities of the carboxylate-derived bands are significantly enhanced.[30]

4. Theoretical Results

The optimized geometries of the benzoate anion, its methyl-substituted isomers, and their corresponding neutrals are shown in Figure 3. A large geometry change was indeed observed between the anions and neutrals for all four species, consistent with the broad PES band observed for the ground states (Figure 1). The largest change in the geometrical parameter between the anions and neutrals is the ∠OCO angle, which has a change of about 19° in all cases: ~129° in the anions versus ~110° in the neutrals. In addition, the C−C bond distance between the $-CO_2$ group and the benzene ring also has a large change, shortening by ~0.08 Å in the neutrals. Except for *o*-$CH_3C_6H_4CO_2^-$ (Figure 3b), the carboxylate groups are all in-plane with the benzene ring. The C−C bond lengths in the ring of the meta- and para-isomers of methyl benzoates are very uniform (1.398−1.403 Å) and are similar to those in the ring of the benzoate in both the anions and the neutrals, suggesting that there are less strains on the ring with the carboxylate and methyl groups being further apart. The carboxylate group in *o*-$CH_3C_6H_4CO_2^-$, however, is rotated ~25° out of the plane of the benzene ring, whereas in the neutral ground state the $-CO_2$ group is in-plane with the benzene ring. The bond length between the two ring carbons to which the carboxylate and methyl groups are attached is 1.416 Å in the anion and 1.415 Å in the neutral, longer than the other C−C bond lengths in the ring, due to the steric effect. The theoretical ADEs predicted for all the anions are also listed and compared with the experimental threshold values in Table 1.

5. Discussion

5.1. Spectral Assignments and Electronic Structures of $C_6H_5CO_2^-$ and Methyl Benzoates. Figure 4 displays the top five valence molecular orbitals (MOs) and their relative orbital energies for benzoate. The top three MOs (HOMO, HOMO-1, HOMO-2) are spaced closely and are clearly oxygen lone pairs on the $-CO_2^-$ group, which are very similar to those in the simplest carboxylate-containing anions.[32,33] These are followed by a large energy gap and two more closely spaced orbitals (HOMO-3 and HOMO-4), which are clearly π orbitals of the ring although HOMO-3 also has some mixing from the carboxylate π orbital. Other valence MOs are much deeply bound and cannot be accessed even at the 157 nm photon energy.[30] This MO pattern is in exact agreement with the observed PES spectra of benzoate. The valence MOs of the

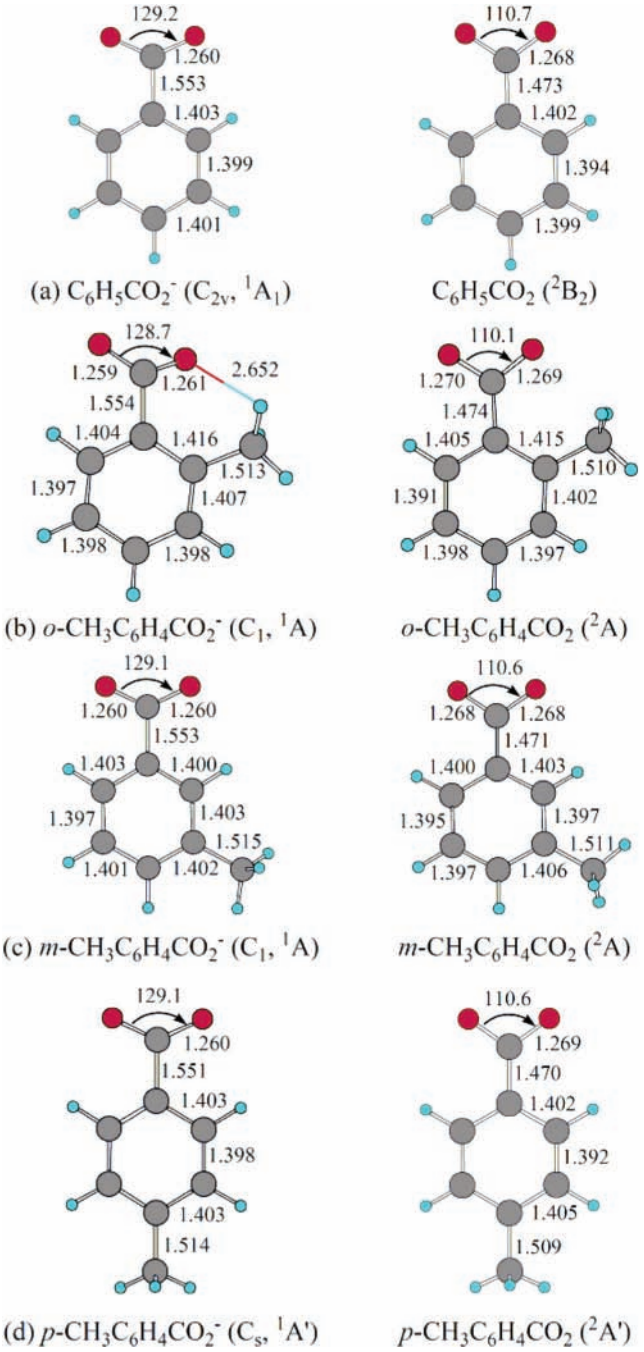

Figure 3. Optimized geometries of (a) $C_6H_5CO_2^-$ and $C_6H_5CO_2$, (b) o-$CH_3C_6H_4CO_2^-$ and o-$CH_3C_6H_4CO_2$, (c) m-$CH_3C_6H_4CO_2^-$ and m-$CH_3C_6H_4CO_2$, and (d) p-$CH_3C_6H_4CO_2^-$ and p-$CH_3C_6H_4CO_2$. Selected bond lengths are given in angstroms and angles are given in degrees.

methyl benzoates should be similar, judging by their similar PES patterns. Only HOMO-3, corresponding to band C in the PES spectra, may be different for the methyl benzoates because this is the only band that appears to be different in the four anions (Figure 2).

The HOMO of benzoate is an antibonding σ orbital from one of the p orbitals on the two oxygen atoms. Thus it is expected that the $\angle$OCO bond angle would be reduced upon removal of an electron from the HOMO. The HOMO also involves a slight antibonding interaction between the carboxylate and the ring, consistent with the shortening of the C−C distance between the carboxylate and the ring in the neutral ground state. The HOMO-1 and HOMO-2 of benzoate involve a σ in-plane bonding combination and an out-of-plane antibonding π orbital, respectively, consistent with the observed OCO bending vibrational progressions for the A and B bands in the PES spectra. The methyl group in the methyl-substituted benzoates should have very little effect to the carboxylate-based MOs, consistent with the very similar PES spectral patterns in the lower binding energy part of the PES spectra for all four species. The lack of vibrational resolution in the o-$CH_3C_6H_4CO_2^-$ isomer is due to the large torsional angle change of the CO_2 group and a steric effect, which will be discussed below. However, the methyl substitution is expected to change the electron density distributions and symmetries of the π MOs of the benzene ring, which in turn would change the activities and excitations of different vibrational modes upon photodetachment, resulting in the differences in bands C and D in PES spectra of the four anions (Figure 2).

5.2. Electron Affinities of the Benzoate Radicals and Experimental TDEs. The EAs of the benzoate radical (C_6H_5-$CO_2^\bullet$) and its methyl-substituted isomers have been deduced in the NIST database[34] using thermodynamic cycles from gas-phase proton-transfer equilibrium measurements.[35,36] The EA values so obtained range from 3.41 eV in p-$CH_3C_6H_4CO_2^-$ to 3.48 eV in o-$CH_3C_6H_4CO_2^-$ with a large uncertainty of $\pm$0.16 eV (Table 1). In principle, the ADEs for the ground-state transitions in our PES data should provide more accurate measures for the EAs. However, as discussed above, due to the large geometry changes between the anion and the neutral ground states, the 0−0 transitions, which define the EAs for the neutral radical species, are likely negligible in the PES spectra for all four anions and only TDEs could be obtained from the PES experiment, which can only serve as upper limits for the ADEs. Indeed, our estimated TDE values are systematically higher than the EAs estimated from the thermodynamic cycles, albeit the large uncertainties ($\pm$0.16 eV) given in the NIST database for the estimated EAs allow sufficient energy ranges to overlap with our estimated TDEs (Table 1).

We have also calculated the EAs for the four species by taking the energy differences between the ground states of the anions and their corresponding neutrals. As shown in Table 1, our calculated EAs are in excellent agreement with the thermodynamically estimated EAs for all but the o-$CH_3C_6H_4CO_2^\bullet$ isomer. Our estimated TDE and calculated EA for this species both yield the lowest value for the o-isomer among the four systems, whereas the thermodynamically estimated EA for the o-isomer seems to be the highest. The lower TDE observed in our experiment and the lower calculated EA value both indicate that the negative charge in the ortho-isomer is destabilized due to the steric effect, as discussed below in more detail. We suspect that the slightly larger EA value estimated for the ortho-isomer from the thermodynamic cycle is not significant considering the large uncertainties. We tentatively conclude that our calculated EAs for the four species are likely closer to the true EAs for the four species.

5.3. Steric Effect and Low Barrier of Internal CO_2 Rotation in o-$CH_3C_6H_4CO_2^-$. The most surprising observation in the current experiment is the lack of vibrational resolution in the spectra of o-$CH_3C_6H_4CO_2^-$ as compared to the other three benzoate species (Figure 1). The similarity of the overall spectral pattern (Figure 1b) of o-$CH_3C_6H_4CO_2^-$ to the other species suggests that these detachment features are all due to the oxygen lone pair orbitals, as shown in Figure 4. At the 300 and 70 K trapping temperatures, the 266 nm spectrum of o-$CH_3C_6H_4CO_2^-$ is rather featureless, in stark contrast to the well-resolved vibrational progressions for the A and B bands in the spectra of the other three species. Even at the lowest temperature of 18

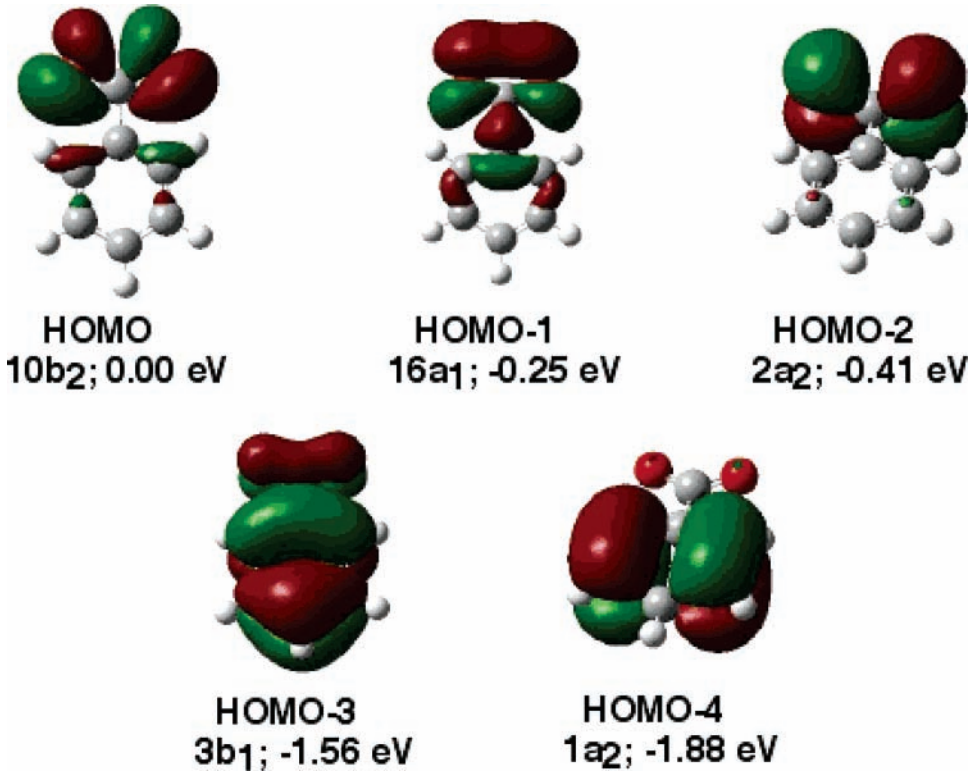

Figure 4. DFT MO contour plots of $C_6H_5CO_2^-$. Orbital symmetries and orbital energies relative to the HOMO are given.

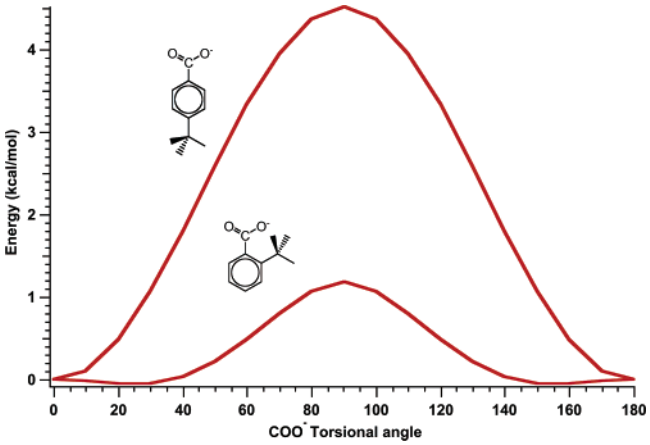

Figure 5. Internal rotational potential energy curves of the $-CO_2^-$ group in (a) *p*-$CH_3C_6H_4CO_2^-$ and (b) *o*-$CH_3C_6H_4CO_2^-$.

K, the A band of *o*-$CH_3C_6H_4CO_2^-$ was still not resolved while the resolution of the B band was improved. This observation suggests that there is a low-frequency vibrational mode in the *o*-$CH_3C_6H_4CO_2^-$ isomer that is difficult to be cooled. As shown from the theoretical calculations (Figure 3), only in the *o*-$CH_3C_6H_4CO_2^-$ isomer the carboxylate group is out-of-plane from the benzene ring. Thus, we considered the internal rotational motion of the carboxylate groups in *p*- and *o*-$CH_3C_6H_4CO_2^-$ to see their differences. Figure 5 displays the calculated internal rotational potential energies and the rotational barriers for the two isomers. Importantly, we found that the $-CO_2^-$ rotational barrier is much larger in *p*-$CH_3C_6H_4CO_2^-$ than in *o*-$CH_3C_6H_4CO_2^-$. The ortho-isomer has an extremely low rotational barrier of ~1 kcal/mol without taking into account the zero point energy. Hence, the $-CO_2^-$ group in *o*-$CH_3C_6H_4CO_2^-$ can be considered a free or hindered rotor even at our lowest ion trap temperature. The internal rotational frequency is expected to be very low and may not be completely cooled even at our lowest trapping temperature of 18 K, corresponding to ~13 cm^{-1}. In addition, the CO_2 torsion angle in the ortho-isomer undergoes a large change from 25° in the anion to 0° in the neutral, which should be mainly responsible for the broad spectrum at 18 K as a result of the coupling between the torsional mode and the OCO bending mode.

5.4. There Is *No* C−H···O Hydrogen Bond in *o*-$CH_3C_6H_4CO_2^-$. A C−H···O hydrogen bond has long been postulated to form between the methyl group and the carboxylate in *o*-$CH_3C_6H_4CO_2^-$ to interpret the stronger acidity of the ortho-isomer relative to the *m*- and *p*-methyl benzoic acids.[5] However, our current experimental and theoretical observations suggest that no such C−H···O hydrogen bond exists. In fact, the methyl-CO_2^- interaction in *o*-$CH_3C_6H_4CO_2^-$ is repulsive in nature. First, we expected that a C−H···O hydrogen bond would stabilize the negative charge on the $-CO_2^-$ group, which should have given rise to higher electron binding energies in the ortho-isomer, as we have observed in the low-temperature PES spectra of $CH_3(CH_2)_nCO_2^-$ with $n > 4$.[25] However, the electron binding energies observed for the *o*-isomer are in fact lower than those in benzoate and are the lowest among the three methyl benzoate isomers. Second, our calculated structures of *o*-$CH_3C_6H_4CO_2^-$ (Figure 3b) shows that the strong steric effect pushes the carboxylate group out of the plane of the benzene ring and lengthens the C−C distance on the ring between the two side groups. Furthermore, the $-CO_2^-$ rotational barrier is significantly reduced due to the steric effect. A C−H···O hydrogen bond would have increased the rotational barrier.

Geometrical criteria have been proposed for the formation of C−H···O hydrogen bonds. The C···O distances were suggested to be smaller than 3.2 Å, and the ∠CHO angles were expected to be between 110° and 180°.[8,9] In the optimized structure of *o*-$CH_3C_6H_4CO_2^-$ (Figure 3b), the C−H···O distance and C−H···O angle from the two CHs in the methyl group are 2.65 Å, 86.8° and 2.47 Å, 96.7°, respectively. Even though the C−H···O distances fall within the nominal range for C−H···O

hydrogen bonding, the ∠CHO angles are much smaller than that expected for C−H···O hydrogen bonding. This result shows that not every close C−H···O contact can form a hydrogen bond. In fact, sometimes close C−H···O contact can indeed be repulsive, which appears to be the case in *o*-$CH_3C_6H_4CO_2^-$.

6. Conclusions

Temperature-dependent and vibrationally resolved photoelectron spectra of benzoate and the three methyl-substituted benzoate anions are reported. Photodetachment features from O lone pairs of the carboxylate and the ring π electrons were observed. The temperature-dependent photoelectron spectra showed that all four anions give similar spectral patterns; $CH_3C_6H_4CO_2^-$, *m*-$CH_3C_6H_4CO_2^-$, and *p*-$CH_3C_6H_4CO_2^-$ yielded well-resolved vibrational structures in the O lone pair region at low temperatures, except for *o*-$CH_3C_6H_4CO_2^-$, which yielded broad spectra even at the lowest ion trap temperature. The ground-state transition in all four species was observed to be broad and poorly resolved, suggesting a large geometry change between the anions and the neutral ground states. Theoretical calculations showed that there is a large ∠OCO bond angle reduction of ∼19° from the anion to neutral ground states in all four species, consistent with the broad spectral features for the ground-state transitions. Strong steric effect was found between the methyl group and the carboxylate group in *o*-$CH_3C_6H_4CO_2^-$, such that the $-CO_2^-$ group is pushed out of the plane of the benzene ring by about 25° and its internal rotational barrier is also significantly reduced. The reduction of the rotational barrier makes *o*-$CH_3C_6H_4CO_2^-$ much more difficult to be vibrationally cooled. And the strong coupling of the CO_2 torsional mode and the OCO bending mode yielded the broad spectra for the ortho-isomer. The present study shows that there is *no* C−H···O hydrogen bond in *o*-$CH_3C_6H_4CO_2^-$.

Acknowledgment. This work was supported by the U.S. Department of Energy (DOE), Office of Basic Energy Sciences, Chemical Science Division. The experiment and calculations were performed at the W. R. Wiley Environmental Molecular Sciences Laboratory, a national scientific user facility sponsored by DOE's Office of Biological and Environmental Research and located at Pacific Northwest National Laboratory, which is operated for DOE by Battelle.

References and Notes

(1) *Steric Effects in Organic Chemistry*; Newman, M. S., Ed.; John Wiley & Sons: New York, 1956.
(2) Hine, J. *Structural Effects on Equilibria in Organic Chemistry*; John Wiley & Sons: New York, 1975.
(3) Charton, M. *Similarity Models in Organic Chemistry, Biochemistry and Related Fields*; Elsevier: Amsterdam, 1991.
(4) Böhm, S.; Fiedler, P.; Exner, O. *New. J. Chem.* **2004**, *28*, 67.
(5) Dippy, J. F. J.; Evans, D. P.; Gordon, J. J.; Lewis; Watson, H. B. *J. Chem. Soc.* **1937**, 1421.
(6) Dippy, J. F. J.; Hughes, S. R. C.; Laxton, J. W. *J. Chem. Soc.* **1954**, 1470.
(7) Mcmahon, T. B.; Kebarle, P. *J. Am. Chem. Soc.* **1977**, *99*, 2222.
(8) Jeffrey, G. A. *An Introduction to Hydrogen Bonding*; Oxford University Press: New York, 1997.
(9) Steiner, T. *Angew. Chem., Int. Ed. Engl.* **2002**, *41*, 48.
(10) Sutor, D. J. *Nature* **1962**, *195*, 68.
(11) Taylor, R.; Kennard, O.; *J. Am. Chem. Soc*. **1982**, *104*, 5063.
(12) Vargas, R.; Garza, J.; Dixon, D. A.; Hay, B. P. *J. Am. Chem. Soc.* **2000**, *122*, 4750.
(13) Gu, Y.; Kar, T.; Scheiner, S. *J. Am. Chem. Soc.* **1999**, *121*, 9411.
(14) Desiraju, G. R. *Acc. Chem. Res.* **1996**, *29*, 441.
(15) Houk, K. N.; Menzer, S.; Newton, S. P.; Raymo, F. M.; Stoddart, J. F.; Williams, D. J. *J. Am. Chem. Soc.* **1999**, *121*, 1479.
(16) May, E.; Destro, R.; Gatti, C. *J. Am. Chem. Soc*. **2001**, *123*, 12248.
(17) Berg, J. A. v. d.; Seddon, K. R. *Cryst. Growth Des*. **2003**, *3*, 643.
(18) Bella, J.; Berman, H. M. *J. Mol. Biol*. **1996**, *264*, 734.
(19) Wahl, M. C.; Rao, S. T.; Sundaralingam, M. *Nature Struct. Biol*. **1996**, *3*, 24.
(20) Berger, I.; Egli, M.; Rich, A. *Proc. Natl. Acad. Sci. U.S.A.* **1996**, *93*, 12116.
(21) Lee, K. M.; Chang, H. C.; Jiang, J. C.; Chen, J. C. C.; Kao, H. E.; Lin, S. H.; Lin, I. J. B. *J. Am. Chem.* Soc. **2003**, *125*, 12358.
(22) Allerhand, A.; Schleyer, P. von P. *J. Am. Chem. Soc.* **1963**, *85*, 1715.
(23) Novoa, J. J.; Tarron, B.; Whangbo, M. H.; William, J. M. *J. Chem. Phys.* **1991**, *95*, 5179.
(24) Wang, X. B.; Woo, H. K.; Barlow, S. E.; Wang, L. S. (in preparation).
(25) Wang, X. B.; Woo, H. K.; Boggavarapu, K.; Wang, L. S. *Angew. Chem., Int. Ed.* **2005**, *44*, 4968.
(26) Wang, L. S.; Ding, C. F.; Wang, X. B.; Barlow, S. E. *Rev. Sci. Instrum.* **1999**, *70*, 1957.
(27) Gilles, M. K.; Polak, M. L.; Lineberger, W. C. *J. Chem. Phys.* **1992**, *96*, 8012.
(28) Becke, A. D. *J. Chem. Phys.* **1993**, *98*, 5648.
(29) Frisch, M. J.; Trucks, G. W.; Schlegel, H. B.; Scuseria, G. E.; Robb, M. A.; Cheeseman, J. R.; Montgomery, J. A., Jr.; Vreven, T.; Kudin, K. N.; Burant, J. C.; Millam, J. M.; Iyengar, S. S.; Tomasi, J.; Barone, V.; Mennucci, B.; Cossi, M.; Scalmani, G.; Rega, N.; Petersson, G. A.; Nakatsuji, H.; Hada, M.; Ehara, M.; Toyota, K.; Fukuda, R.; Hasegawa, J.; Ishida, M.; Nakajima, T.; Honda, Y.; Kitao, O.; Nakai, H.; Klene, M.; Li, X.; Knox, J. E.; Hratchian, H. P.; Cross, J. B.; Bakken, V.; Adamo, C.; Jaramillo, J.; Gomperts, R.; Stratmann, R. E.; Yazyev, O.; Austin, A. J.; Cammi, R.; Pomelli, C.; Ochterski, J. W.; Ayala, P. Y.; Morokuma, K.; Voth, G. A.; Salvador, P.; Dannenberg, J. J.; Zakrzewski, V. G.; Dapprich, S.; Daniels, A. D.; Strain, M. C.; Farkas, O.; Malick, D. K.; Rabuck, A. D.; Raghavachari, K.; Foresman, J. B.; Ortiz, J. V.; Cui, Q.; Baboul, A. G.; Clifford, S.; Cioslowski, J.; Stefanov, B. B.; Liu, G.; Liashenko, A.; Piskorz, P.; Komaromi, I.; Martin, R. L.; Fox, D. J.; Keith, T.; Al-Laham, M. A.; Peng, C. Y.; Nanayakkara, A.; Challacombe, M.; Gill, P. M. W.; Johnson, B.; Chen, W.; Wong, M. W.; Gonzalez, C.; Pople, J. A. *Gaussian 03*, revision B.04; Gaussian, Inc.: Wallingford, CT, 2004.
(30) Wang, X. B.; Nicholas, J. B.; Wang, L. S. *J. Chem. Phys.* **2000**, *113*, 653.
(31) Wang, X. B.; Woo, H. K.; Wang, L. S. *J. Chem. Phys.* **2005**, *123*, 051106.
(32) Kim, E. H.; Bradforth, S. H.; Arnold, D. W.; Metz, R. B.; Neumark, D. M. *J. Chem. Phys.* **1995**, *103*, 7801.
(33) Lu, Z.; Continetti, R. E. *J. Phys. Chem. A* **2004**, *108*, 9962.
(34) The NIST Chemistry WebBook (http://webbook.nist.gov/chemistry/).
(35) McMahon, T. B.; Kebarle, P. *J. Am. Chem. Soc*. **1977**, *99*, 2222.
(36) Fujio, M.; McIver, Jr., R. T.; Taft, R. W. *J. Am. Chem. Soc*. **1981**, *103*, 4017.